Progress In Electromagnetics Research, Vol. 163, 107–117, 2018

Subarray Design for C-Band Circularly-Polarized Synthetic Aperture Radar Antenna Onboard Airborne

Cahya Edi Santosa[1, 2, *], Josaphat T. Sri Sumantyo[1], Chua Ming Yam[1], Katia Urata[1], Koichi Ito[3], and Steven Gao[4]

Abstract—This paper presents the design and realization of a 4×4 broadband circularly polarized microstrip antenna as subarray element for airborne C-band circularly polarized synthetic aperture radar (CP-SAR). The main objective of this work is to optimize impedance bandwidth, axial-ratio bandwidth, gain, and radiation pattern of a CP-SAR array antenna due to the limitation in the available space for a large array antenna installation on airborne platform. Various patch separations in uniformly 2×2 subarray configuration have been simulated to investigate characteristics of impedance bandwidth, axial-ratio bandwidth, gain, and radiation pattern. In order to broaden impedance bandwidth, the proposed antenna is constructed by stacking two thick substrates with low dielectric constant and dissipation factor. The measured 10-dB impedance bandwidth is 0.91 GHz (17.2%), spanning from 4.83 GHz to 6.01 GHz. A simple square patch with curve corner-truncation is applied as the main radiating patch for circularly-polarized wave generation. The radiating patch is excited by single-fed proximity coupled strip-line feeding. The improvement of axial-ratio bandwidth in 2×2 and 4×4 subarray is employed by a feeding network with serial-sequential-rotation configuration. Experimental result shows the 3-dB axial-ratio bandwidth achieved 1.18 GHz (22.17%) from 4.8 GHz to 5.71 GHz. Other characteristic parameters such as gain and radiation pattern of the 4×4 subarray antenna are also presented and discussed.

1. INTRODUCTION

Synthetic aperture radar (SAR) is an active imaging radar that transmits electromagnetic wave and receives the scattering wave from the object. As an active imaging radar, SAR system allows to be operated in all weather conditions such as cloudy, foggy, or day to night time [1]. Many SAR systems have been operated in linearly-polarized (LP) microwave mode (VV, HH, VH, and HV) with high RF power [2]. Unfortunately, LP microwaves is sensitive to Faraday rotation when the wave propagates through the ionosphere. The orientation angle of the LP microwave is changed and needs to be corrected [3]. This issue could be neglected by using circularly-polarized (CP) antennas [4, 5].

The microstrip antenna is a reasonable candidate for developing large array antennas of CP-SAR sensor. It has attractive features of compact size, light weight, and low fabrication cost. However, microstrip antennas have drawbacks as narrow bandwidth, low efficiency, and low gain [6–8]. The common strategy to develop large array antennas for CP-SAR sensor employs a subarray as an element of the large array antenna [9]. In this technique, the design is focused on the optimization of a small subarray and duplicating it in a large array configuration. In order to achieve the CP-SAR antenna requirements, repeating element into large array configuration is physically constrained due to the size

Received 6 June 2018, Accepted 28 August 2018, Scheduled 24 September 2018
* Corresponding author: Cahya Edi Santosa (maxedi77@gmail.com).
[1] Center for Environmental Remote Sensing (CEReS), Chiba University, Japan. [2] Center for Aeronautics Technology, National Institute of Aeronautics and Space, Bogor, Indonesia. [3] Research Center for Frontier Medical Engineering, Chiba University, Japan. [4] Department of Engineering and Digital Arts, University of Kent, Centerbury CT2 7NZ, UK.

and type of the CP-SAR system platform. Undesirable grating lobe and side lobe that may appear in the large array design and also needs to be suppressed [10, 11].

Most studies in CP microstrip antennas technology focus on broadening the impedance bandwidth (IBW), axial-ratio bandwidth (ARBW), and gain. A broad IBW can be reached by increasing the substrate thickness, decreasing the dielectric constant of the substrate, and constructing the antenna on thick multi-layered substrates [12, 13]. Serial-sequential-rotation (SSR) technique has been introduced on CP subarray configuration for ARBW improvement [14]. In [15] application of the SSR principle on subarray obtains approximately 47.8% of ARBW. In addition, implementation of parasitic patches to enhance a high peak gain and also has been investigated in [16].

Recently, Center for Environmental and Remote Sensing (CEReS), Chiba University, Japan, is developing airborne C-band CP-SAR system to observe disaster and environmental changes [17]. The specification of the airborne C-band CP-SAR sensor is listed in Table 1. Previously, the design of C-band CP-SAR antenna has been proposed, but neither IBW nor ARBW meets the requirements of the CP-SAR system, which is less than 5% [18]. In this paper, a new design of 4×4 broadband circularly polarized microstrip antenna as subarray element for the airborne C-band CP-SAR sensor will be presented. The single patch antenna as a basic element of this subarray has been proposed in [19]. Total gain of the antenna will be improved by increasing the number of subarrays on a large array developing. This paper is organized as follows: Section 2 describes the single patch antenna and arraying techniques to broaden IBW and ARBW. Section 3 presents the prototype of 4×4 subarray and experimental verification. Finally, the findings are concluded in Section 4.

Table 1. Specifications of the array antenna for C-band airborne CP-SAR.

Parameter	Value	Parameter	Value
Center frequency (f_c)	5.3 GHz	Total gain	> 20 dBic
Impedance bandwidth	400 MHz (7.6%)	Side-lobe-level	-20 dB
3 dB axial-ratio bandwidth	400 MHz (7.6%)	VSWR	1.5
Range beam-width	10° (E-plane)	Input impedance	50 Ω
Azimuth beam-width	5° (H-plane)	Dimension	500 mm × 300 mm × 10 mm

2. DESIGN OF ANTENNA

The airborne CP-SAR array antenna is designed for RF transmitter (TX) and receiver (RX) with both right-handed circularly polarized (RHCP) and left-handed circularly-polarized (LHCP) modes. Fig. 1(a)

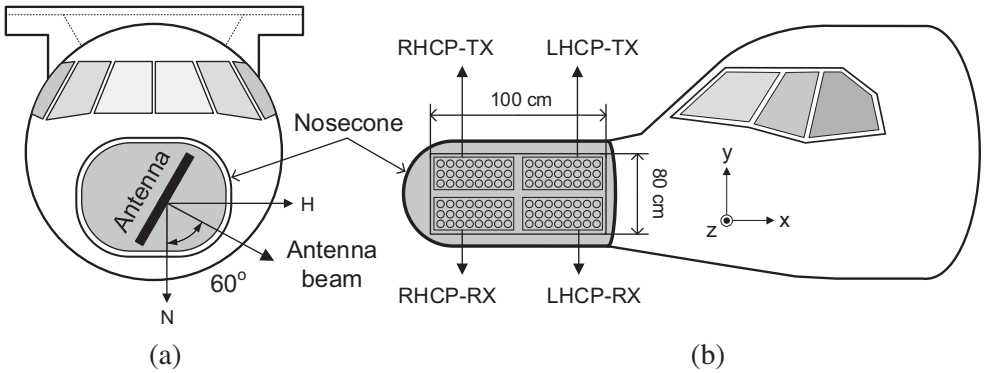

Figure 1. Layout of the airborne CP-SAR antenna that is installed inside the nosecone of CN-235 aircraft. (a) Direction of the antenna (off-nadir-angle: 60°). (b) Configuration of the antenna for full-polarimetric mode.

illustrates the layout of side looking CP-SAR array antenna that is installed inside the nosecone of the CN-235 aircraft. The direction of the main beam of the antenna towards nadir axis (N) is approximately 60°. Fig. 1(b) shows the configuration of full-polarimetric mode (RR, LL, RL, and LR) of the airborne CP-SAR sensor. Available space inside the nosecone of the aircraft is 100 cm of length in x-axis and 80 cm of width in y-axis. Limitation in space is a challenge for array antenna design to achieve the optimum performance of IBW, ARBW, and gain.

2.1. Single Patch

The structure of the single patch antenna is illustrated in Fig. 2(a). The proposed antenna is designed with double-stacked substrate of 1.6 mm thickness (h), 2.17 dielectric constant (ϵ_r), and 0.0005 dissipation factor ($\tan d$-δ). The thick substrate with low dielectric constant is selected in order to broaden the IBW. Circular polarization is generated by a square patch with diagonally curve corner-truncation placed between the substrates which is fed by a single-feed proximity-coupled microstrip line. A circle-slotted parasitic patch is added to the above on the radiating patch in order to improve the ARBW and gain. The upper layer of the top substrate is covered by copper to reduce undesired electromagnetic field emitted by the feeding. The detailed geometry of the single patch antenna is shown in Fig. 2(b), and the dimension is listed in Table 2.

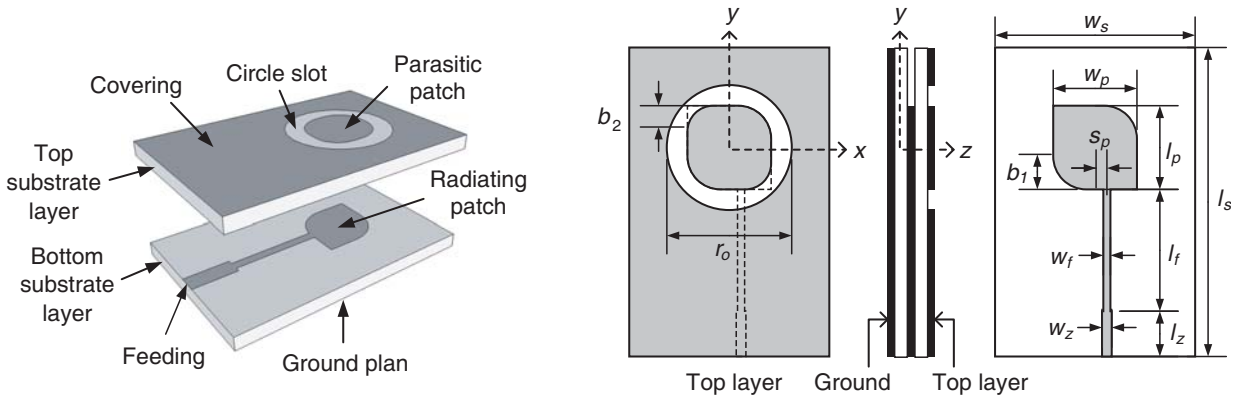

Figure 2. Structure of the single patch antenna. (a) 3D view. (b) Detailed geometry.

Table 2. Dimension of the single patch antenna.

Variable	Length (mm)	Variable	Length (mm)	Variable	Length (mm)
w_s	42.4	l_s	65.5	s_p	2.5
w_p	17.8	l_p	17.8	r_o	26.5
w_f	1.5	l_f	25.8	b_1	7.0
w_z	2.0	l_z	9.6	b_2	5.5

Figure 3 shows the comparison between simulated characteristics and measured performance of the single patch antenna. The simulated and measured IBWs, ARBWs, gains, and VSWRs are illustrated in Fig. 3(a), Fig. 3(b), Fig. 3(c), and Fig. 3(d), respectively. The desired operational bandwidth of the airborne CP-SAR array antenna system is shown by the shadowed-bar in the frequency axis. Several efforts to improve characteristics of the single patch antenna have been discussed in [19].

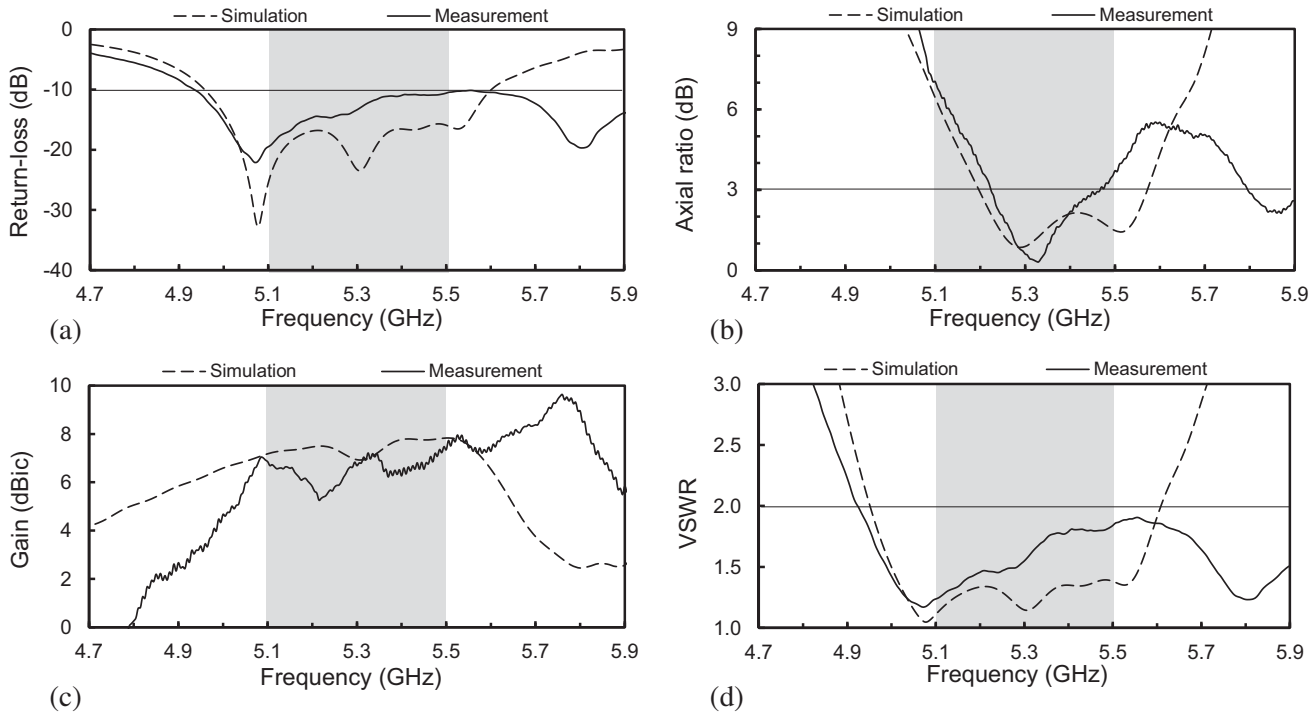

Figure 3. Simulated and measured characteristic of the single patch antenna. (a) Return-loss (S_{11}), (b) axial-ratio, (c) gain, and (d) VSWR.

2.2. A 2 × 2 Subarray

2.2.1. Impedance Matching

The subarray elements employ a 2 × 2 configuration with SSR principle as an effort to broaden the IBW and ARBW. The design of impedance matching for the 2 × 2 subarray feeding network with SSR configuration is shown in Fig. 4(a). Each subarray element (patch 1 until patch 4) is fed by stripline feeding that is matched to 100 Ω. T-junction power divider is applied to obtain uniformly power distribution. Quarter-lambda ($\lambda/4$) microstrip line is applied as 90° phase shifter between one patch and another patch to perform SSR configuration.

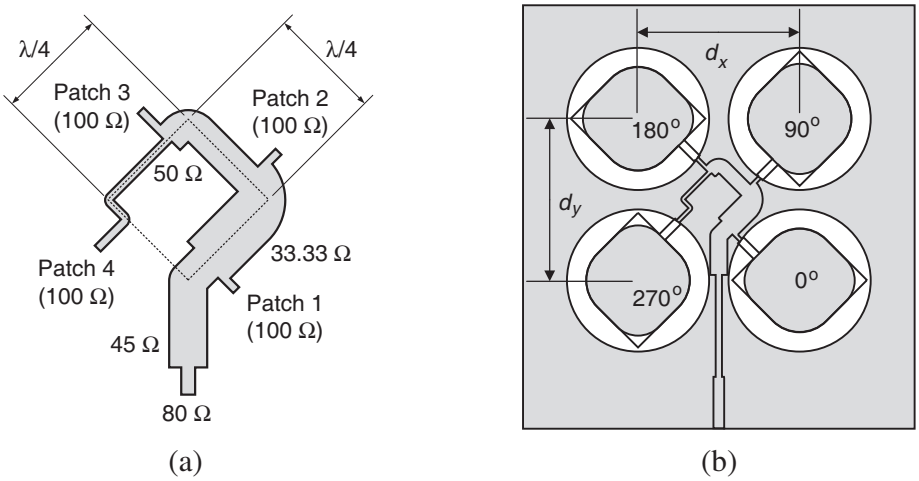

Figure 4. The 2 × 2 subarray configuration. (a) Impedance matching for SSR feeding network. (b) Separation and 90° phase differences between each patch.

2.2.2. Patch Separation

Figure 4(b) illustrates the 2×2 subarray configuration with patch separation d_x (in x-axis) and d_y (in y-axis). Quarter-lambda ($\lambda/4$) microstrip line on feeding network creates 90° phase differences between array elements to implement the SSR principle. The patch separation among array elements is chosen between $0.5\lambda_o$ and $1.0\lambda_o$ to avoid unintended beam of radiation pattern in the array antenna, where λ_o is a wavelength in free space [20]. For optimization study, several uniform patch separations ($d_x = d_y$) in $0.5\lambda_o$, $0.6\lambda_o$, $0.7\lambda_o$ are simulated and discussed.

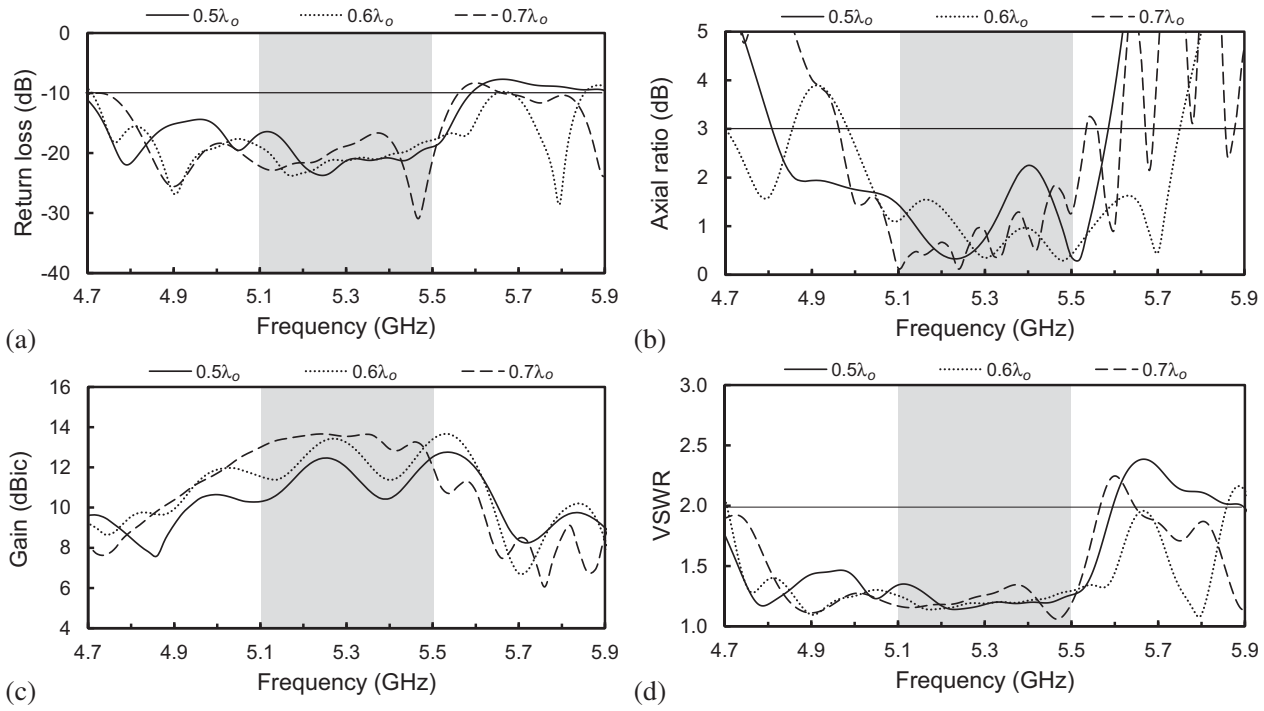

Figure 5. Characteristics of the 2×2 subarray configuration in uniformly patch separation ($d_x = d_y$) for $0.5\lambda_o$, $0.6\lambda_o$, and $0.7\lambda_o$. (a) Return loss (S_{11}). (b) Axial ratio. (c) Gain. (d) VSWR.

Figure 5 shows the simulated characteristic of the 2×2 subarray with SSR configuration in several uniform patch separations at the center frequency of 5.3 GHz. Fig. 5(a), Fig. 5(b), Fig. 5(c), and Fig. 5(d) depict the return-loss, axial-ratio, gain, and VSWR, respectively. The desired operational bandwidth of the airborne CP-SAR array antenna is shown by the shadowed-bar in the frequency axis. It is clearly shown that the IBW and ARBW have been broadened after SSR configuration with uniform patch separation applied in the antenna arraying. Both IBW and ARBW have fulfilled the requirements of the airborne CP-SAR array antenna. The peak gain of the 2×2 subarray fluctuats from 10 dBic to 13.5 dBic along the operational frequency. The total gain will be improved by increasing the number of patch elements into large array configuration. The trend of VSWR indicates that the feeding network has excellent matching impedance along the operational bandwidth with VSWR value under 1.5 in all uniformly patch separation.

The detailed characteristics of the 2×2 subarray antenna with SSR configuration in some patch separations ($0.5\lambda_o$, $0.6\lambda_o$, $0.7\lambda_o$) are listed in Table 3. Compared to the 2×2 subarray with patch separation $0.5\lambda_o$ and $0.6\lambda_o$, the 2×2 subarray with patch separation of $0.7\lambda_o$ has better gain, more flat distribution of gain along operational frequency, narrower beamwidth (BM) in both H-plane and E-plane, and is closer to $\theta = 0°$ in direction of main-lobe. Unfortunately, the estimation dimension for 16×8 array configuration with uniform patch separation $0.7\lambda_o$ exceeds the requirement. The length of the 16×8 array antenna in x-axis exceeds 50 cm with total length of 64 cm. Moreover, it has the worst character in the IBW, ARBW and side-lobe-level (SLL). On the other hand, the 2×2 subarray with

Table 3. Characteristics of the 2×2 subarray with SSR configuration in some values of patch separation that simulated at the center frequency of 5.3 GHz.

Parameters		$d_x = d_y = 0.5\lambda_o$	$d_x = d_y = 0.6\lambda_o$	$d_x = d_y = 0.7\lambda_o$	Unit
Return-loss (S_{11})	f_L	4.68	4.71	4.67	GHz
	f_H	5.59	5.65	5.56	GHz
	IBW	910 (17.17)	940 (17.74)	890 (16.79)	MHz (%)
Axial-ratio (AR)	f_L	4.81	4.98	4.96	GHz
	f_H	5.58	5.75	5.54	GHz
	ARBW	770 (14.53)	770 (14.53)	580 (10.94)	MHz (%)
H-plane ($\phi = 0°$)	Direction	6.0	3.0	2.0	Degree
	BM	44.20	38.30	33.40	Degree
	SLL	−18.20	−16.00	−11.90	dB
E-plane ($\phi = 90°$)	Direction	0.0	0.0	0.0	Degree
	BM	43.50	38.40	33.40	Degree
	SLL	−28.80	−20.40	−11.8	dB
Gain		12.00	13.23	13.54	dBic
VSWR (1 : 2)		1.2	1.2	1.2	None
Dimension of 16×8 array ($x \times y$)		471.5×245.2	556.3×284.8	641×324.4	mm

patch separation $0.5\lambda_o$ has better attributes in broad IBW and ARBW, lower SLL, and more compact size for the 16×8 array configuration with 47 cm of length in x-axis, so that the subarray with patch separation $0.5\lambda_o$ has more possibility to be realized.

2.3. A 4×4 Subarray

The 4×4 subarray employs the uniformly patch separation $0.5\lambda_o$ with fully-serial-sequential-rotation (FSSR) technique in RHCP mode with phase arrangement as shown in Fig. 6. The 4×4 subarray is

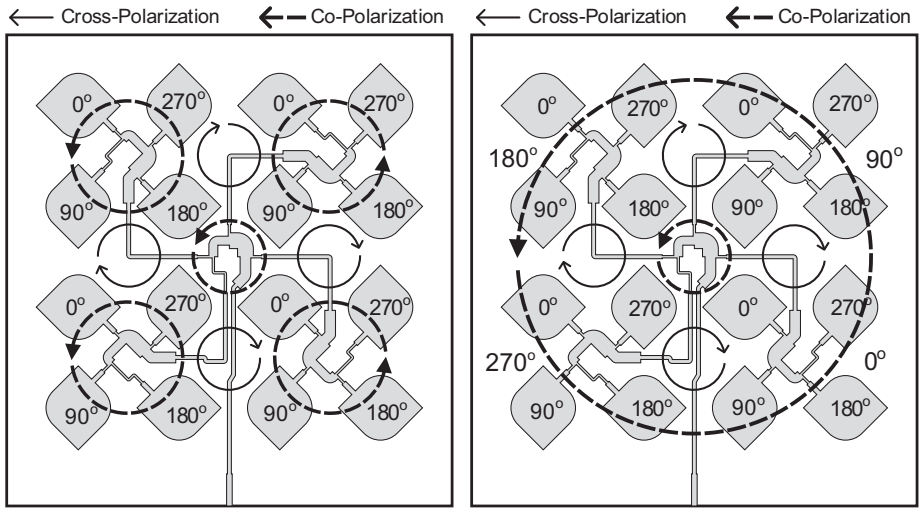

Figure 6. Phase arrangement of the 4×4 subarray configuration with co-polarization and cross-polarization rotation consideration. (a) SSR. (b) FSSR.

arranged by 4 sets of the 2×2 subarray configuration in which each set of the 2×2 subarray applies SSR principle in RHCP rotation as illustrated in Fig. 6(a). Every first patch (patch 1) in the SSR configuration of the 2×2 subarray is placed as the central element of the 4×4 subarray configuration. Quarter-lambda phase shifter of the 4×4 subarray feeding network makes 90° phase differences between four patches in the center position (every patch 1 of the 2×2 subarray). This configuration performs co-polarization rotation at the center element of the 4×4 subarray and cross-polarization between sets of the 2×2 subarray. Fig. 6(b) illustrates the FSSR principle in RHCP mode composed by 4 sets of 2×2 subarray configuration. Quarter-lambda phase shifter of the 4×4 subarray feeding network makes 90° phase differences between sets to perform co-polarization rotation.

3. EXPERIMENTAL VALIDATION OF 4×4 SUBARRAY

The 4×4 subarray antenna that employs the uniform patch separation $0.5\lambda_o$ with FSSR configuration is fabricated, measured, and shown in Fig. 7. The top view of the prototype antenna with circle-slotted parasitic patch antenna is shown in Fig. 7(a), and the feeding network with FSSR configuration is shown in Fig. 7(b). The printed substrates are then stacked and fixed by 2 mm plastic screws at several locations. The dimension of the fabricated antenna is approximately 132 mm × 132 mm × 3.3 mm (length × width × thickness) and fed by 50 Ω female SMA connector.

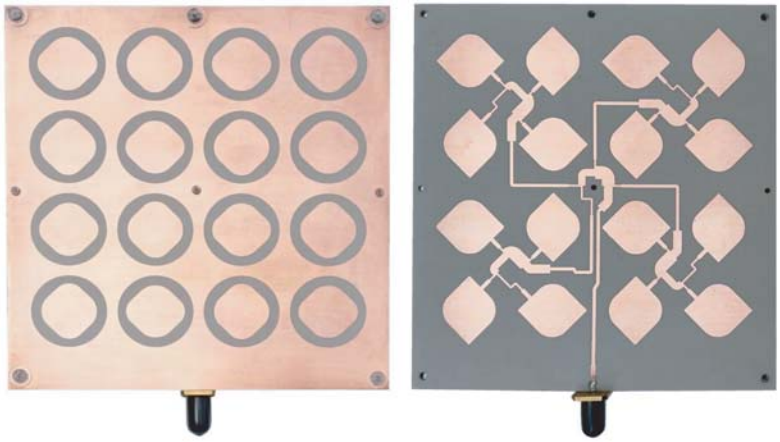

(a) (b)

Figure 7. The realized of the 4×4 subarray antenna with RHCP configuration. (a) Top view with circle-slotted parasitic patch. (b) Feeding network with FSSR configuration.

The performance of the 4×4 subarray antenna is measured in an anechoic chamber using E8364C PNA Microwave Network Analyzer. Fig. 8 shows the comparison result between the measured performance and simulated characteristics of the prototype antenna. The desired operational bandwidth of the airborne CP-SAR array antenna is shown by the shadowed-bar in the frequency axis. Fig. 8(a), Fig. 8(b), Fig. 8(c), and Fig. 8(d) plot the return-loss, axial-ratio, gain, and VSWR, respectively. The graph clearly shows that the IBW and ARBW of the prototype antenna have fulfilled the requirements. The measured IBW is approximately 910 MHz (17.17%) spanning from 4.80 GHz to 5.71 GHz. The measured ARBW is approximately 1180 MHz (22.17%) spanning from 4.83 GHz to 6.01 GHz. The measured gain distribution along operational bandwidth is not flat but has similar trends to the simulation results. The minimum gain is measured 13.2 dBic at frequency 5.22 GHz; the maximum gain is 16.96 dBic at frequency 5.42 GHz; the average gain is 15.0 dBic at the center frequency of 5.3 GHz. The characteristic of VSWR along the operational bandwidth also presents a good performance, and approximately 62.5% of operational bandwidth has VSWR lower than 1.5 spreading from 5.25 GHz to 5.5 GHz.

Figure 9 shows the simulated and measured radiation patterns of the 4×4 subarray configuration

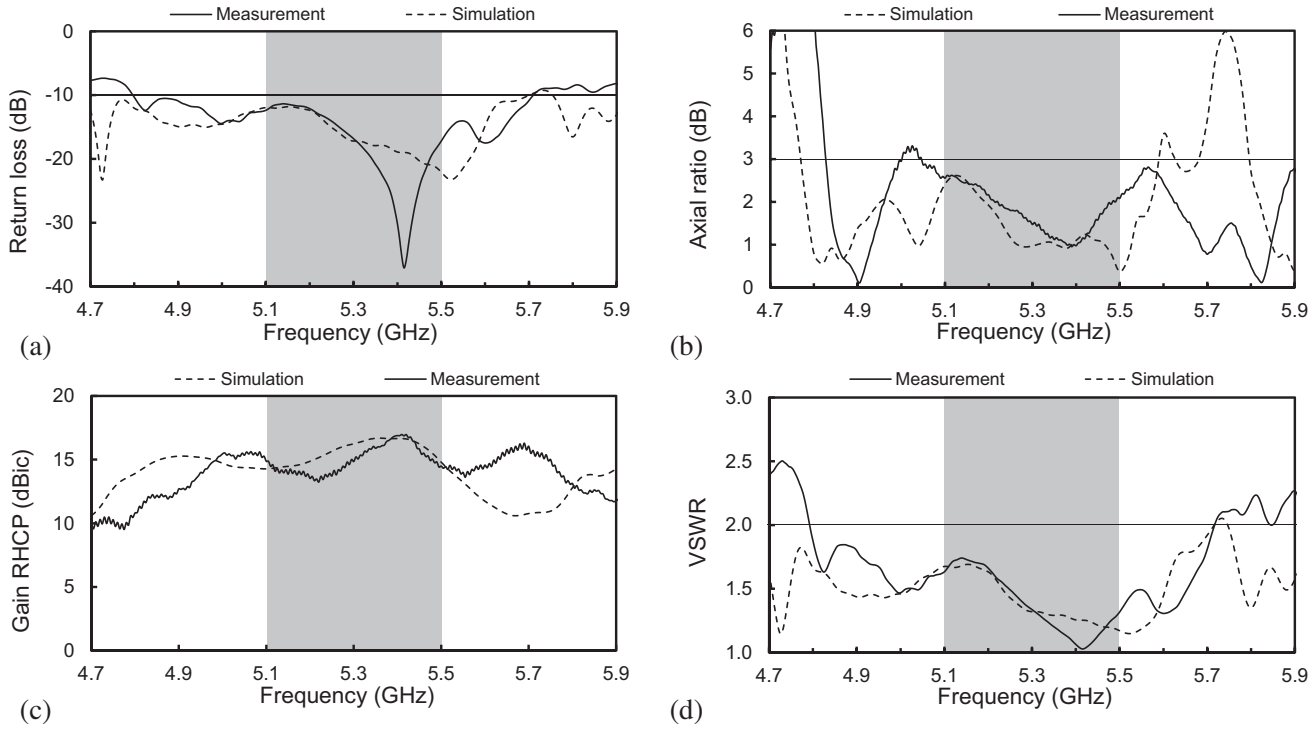

Figure 8. Comparison result between simulation and measurement of the 4×4 subarray antenna with FSSR configuration. (a) Return loss. (b) Axial ratio. (c) Gain. (d) VSWR.

Table 4. Measured characteristics of the 4×4 subarray antenna with patch separation $d_x = d_y = 0.5\lambda_o$ in RHCP configuration.

Parameters		Value		Unit
		Simulation	Measurement	
Return-loss (S_{11})	f_L	4.69	4.80	GHz
	f_H	5.70	5.71	GHz
	IBW	1010 (19.14)	910 (17.17)	MHz (%)
Axial-ratio (AR)	f_L	4.77	4.83	GHz
	f_H	5.69	6.01	GHz
	ARBW	910 (17.19)	1180 (22.17)	MHz (%)
H-plane ($\phi = 0°$)	Direction	3.0	4.0	Degree
	BM	22.5	22.0	Degree
	SLL	-7.9	-8.0	dB
E-plane ($\phi = 90°$)	Direction	0.0	0.0	Degree
	BM	23.4	23.0	Degree
	SLL	-13.6	-12.0	dB
Gain		15.4	15.0	dBic
VSWR (1 : 2)		1.3	1.3	None
Dimension ($x \times y$)		132.0×132.0	132.0×132.0	mm

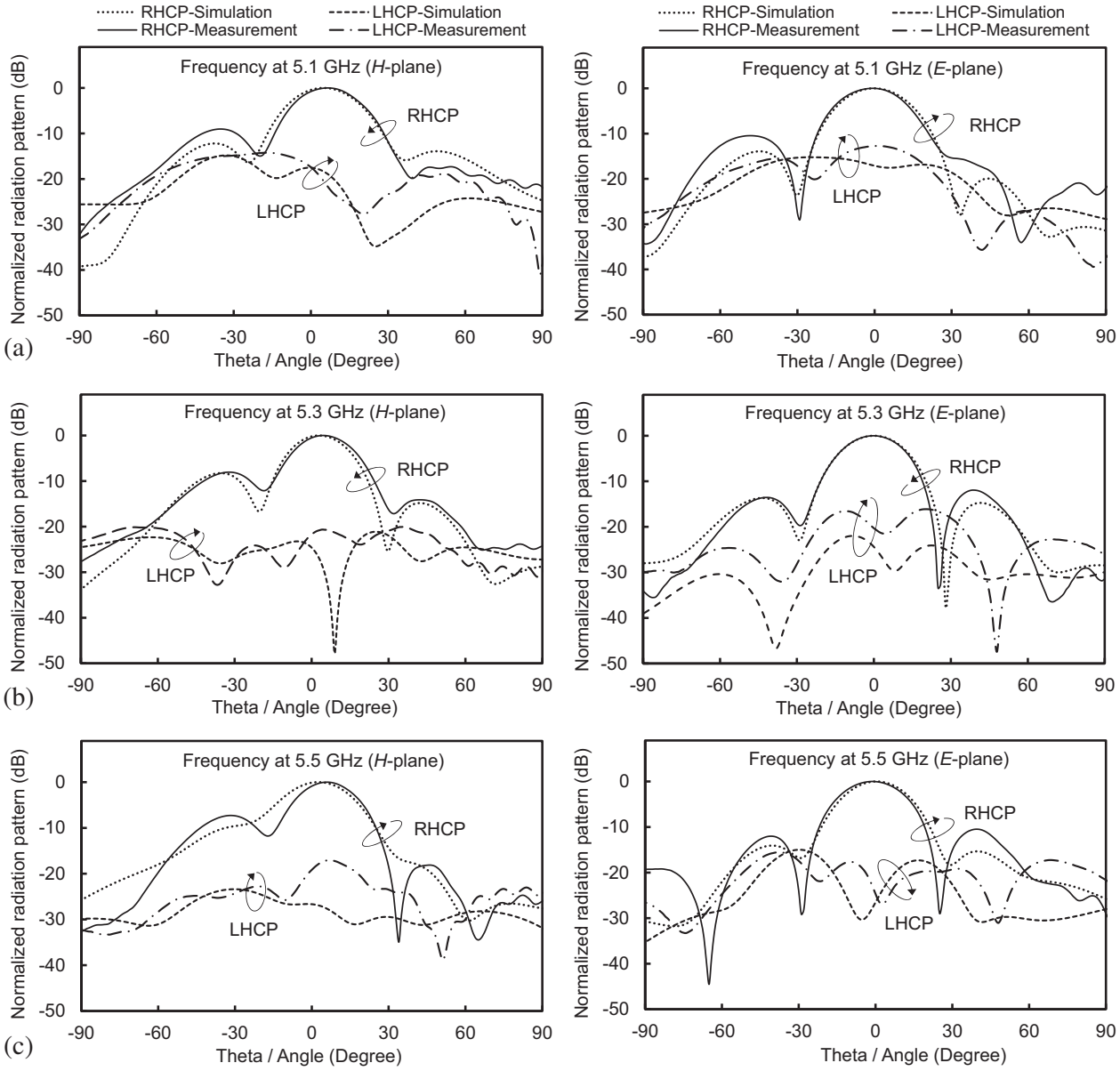

Figure 9. The simulated and measured radiation pattern of 4×4 subarray antenna in H-plane and E-plane at monitoring frequency: (a) 5.1 GHz. (b) 5.3 GHz. (c) 5.5 GHz.

in H-plane and E-plane. The normalized radiation patterns as a function of co-polarization (RHCP) and cross-polarization (LHCP) at monitoring frequencies 5.1 GHz, 5.3 GHz, and 5.5 GHz are plotted in Fig. 9(a), Fig. 9(b), Fig. 9(c), respectively. In H-plane at all monitoring frequencies, the first side-lobe appears at theta $-32°$ and theta $42°$ with maximum SLL -8.0 dB and -14 dB. On the other hand, the first side-lobe in E-plane at all monitoring frequencies comes out at theta $-35°$ and theta $39°$ with maximum SLL -9.0 dB and -12 dB. In order to avoid a problem on CP-SAR image processing due to undesirable noise from side-lobe scattering, the side-lobe-level of CP-SAR array antenna in H-plane needs to be taken care of. The prototype antenna has a main-lobe direction at $4°$ in H-plane and $0°$ in E-plane where both directions have cross-polarization level approximately in -20 dB at all monitoring frequency.

Table 4 summarizes measured characteristics of the realized antenna compared to the simulation performance at the monitoring frequency of 5.3 GHz. The table shows that the realized antenna has

good performance. Some measurement results were not in accordance with simulation results due to unavoidable errors in fabrication and measurement process such us under/over-etching, misalignment the combination between the top substrate and bottom substrate, and inhomogeneity during fabrication of the double-stacked substrate construction that consists partly of dielectric material and partly of air.

4. CONCLUSION

The 4×4 subarray antenna employing the uniform patch separation of $0.5\lambda_o$ with FSSR configuration is simulated, fabricated, measured and discussed. A broad IBW, ARBW, and optimum gain have been achieved by using a thick substrate with low dielectric constant, double-stacked substrate structure, employing FSSR configuration, and adding circle-slotted parasitic patch above the radiating patch. The subarray with patch separation of $0.5\lambda_o$ gives excellent attributes in the broad IBW and ARBW, low SLL, and compact size which fulfill almost all requirements of the CP-SAR antenna. Parameters of the proposed antenna, which have not fulfilled the requirements, such as low gain, wide BM, and asymmetrical main-lobe direction at 0-degree, will be solved by duplicating the number of subarrays. In future work, the subarray antenna will be arranged to a 16×8 array configuration in order to achieve the total gain more than 20 dBic and narrow BM in both H-plane and E-plane accordance with the airborne CP-SAR sensor requirements.

ACKNOWLEDGMENT

Josaphat Laboratory (JMRSL) is supported in part by the European Space Agency (ESA) Earth Observation Category 1 under Grant 6613, the 4th Japan Aerospace Exploration Agency (JAXA) ALOS Research Announcement under Grant 1024, the 6th JAXA ALOS Research Announcement under Grant 3170, the Japanese Government National Budget Ministry of Education and Technology (MEXT) FY2015-2017 under Grant 2101, Chiba University Strategic Priority Research Promotion Program FY2016-FY2018, Taiwan National Space Organization (NSPO) FY2017-FY2018, SOAR-EI Canadian Space Agency (CSA) Project 5436 FY2017-FY2019, and Indonesian National Institute of Aeronautics and Space (LAPAN).

REFERENCES

1. Curlander, J. C. and R. N. McDonough, *Synthetic Aperture Radar System and Signal Processing*, A John Willey and Sons Inc., Canada, 1991.
2. Ouchi, K., "Recent trend and advance of synthetic aperture radar with selected topics," *Remote Sensing*, 716–807, 2013.
3. Gail, W. B., "Effect of faraday rotation on polarimetric SAR," *IEEE Int. Transaction on Aerospace and Electronic System*, Vol. 34, 301–307, 1998.
4. Sri Sumantyo, J. T., K. V. Chet, L. T. Sze, T. Kawai, T. Ebinuma, Y. Izumi, M. Z. Baharuddin, S. Gao, and K. Ito, "Development of circular polarized synthetic aperture radar onboard UAV JX-1," *International Journal of Remote Sensing*, Vol. 38, 2745–2756, 2017.
5. Gao, S., Q. Luo, and F. Zhu, *Circularly Polarized Antenna*, John Willey and Sons, 2014.
6. Balanis, C. A. *Antenna Theory Analysis and Design*, 3th Edition, John Wiley and Sons, New Jersey, 2005.
7. James, J. R. and P. S. Hall, *Handbook of Microstrip Antennas*, Peter Peregrinus Ltd, London, UK, 1989.
8. Carver, K. R. and J. W. Mink, "Microstrip antenna technology," *IEEE Transactions on Antennas and Propagation*, Vol. 29, No. 1, 2–24, 1981.
9. Granholm, J. and K. Woelders, "Microstrip antenna array for airborne high-performance, polarimetric SAR system," *Symposium on Antennas Technology and Applied Electromagnetics*, 643–650, 1998.

10. Brockett, T. J. and Y. R. Samii, "Subarray design diagnostics for the suppression of undesirable grating lobes," *IEEE Transactions on Antennas and Propagation*, Vol. 60, No. 3, 1373–1380, 2012.
11. Pozar, M. D. and B. Kaufman, "Design consideration for low sidelobe microstrip arrays," *IEEE Transactions on Antennas and Propagation*, Vol. 38, No. 8, 1176–1185, 1990.
12. Davidson, K., Y. Antar, and A. Freundorfer, "A wideband via fed circularly polarized microstrip antenna on a multi-layer substrate," *IEEE Antennas and Propagation Society International Symposium*, APS-URSI, 2013.
13. Yang, W., J. Zhou, Z. Yu, and L. Li, "Single-fed low profile broadband circularly polarized stacked patch antenna," *IEEE Transactions on Antennas and Propagation*, Vol. 62, No. 10, 5406–5410, 2014.
14. Hall, P. S., J. S. Dahele, and J. R. James, "Design principles of sequentially fed, wide bandwidth, circularly polarized microstrip antennas," *IEE Proceedings H — Microwaves, Antennas, and Propagation*, Vol. 136, 381–389, 1989.
15. Hu, Y. J., W. P. Ding, and W. Q. Cao, "Broadband circularly polarized microstrip antenna using sequentially rotated technique," *IEEE Antennas and Wireless Propagation Letters*, Vol. 10, 1358–1361, 2011.
16. Ding, K., C. Gao, T. Yu, D. Qu, and B. Zhang, "Gain-improved broadband circularly polarized antenna array with parasitic patches," *IEEE Antennas and Wireless Propagation Letters*, Vol. 16, 1468–1471, 2017.
17. Sumantyo, J. T. S., "Progress on development of synthetic aperture radar onboard UAV and microsatellite," *IEEE International Geoscience and Remote Sensing Symposium*, 1081–1084, 2014.
18. Baharuddin, M. Z. and J. T. S. Sumantyo, "Suppressed side-lobe, beam steered, C-band circular polarized array antenna for airborne synthetic aperture radar," *Journal of Unmanned System Technology*, Vol. 4, No. 1, 2016.
19. Edi Santosa, C. and J. T. Sri Sumantyo, "Development of a low profile wide-bandwidth circularly polarized microstrip antenna for C-band airborne CP-SAR sensor," *Progress In Electromagnetics Research C*, Vol. 81, 77–88, 2018.
20. Hansen, R. C., *Phased Array Antennas*, John Wiley and Sons, 1998.